



Development and Characterization of Thujone Loaded Pegylated Nanoparticle Delivery for Enhanced Brain Targeting

Dev Sharan Chaturvedi^{1*} Ramteke Kuldeep Hemraj² Dharmendra Singh Rajput³ Naveen Gupta⁴

1. Ph.D. Research Scholar, Patel College of Pharmacy, Madhyanchal Professional University, Bhopal
2. Professor, Patel College of Pharmacy, Madhyanchal Professional University, Bhopal
3. Professor, Patel College of Pharmacy, Madhyanchal Professional University, Bhopal
4. Professor, Patel College of Pharmacy, Madhyanchal Professional University, Bhopal

Dev Sharan Chaturvedi (Corresponding Author)

(Received: 14 April 2024

Revised: 1 May 2024

Accepted: 18 June 2024)

KEYWORDS

Alzheimer's disease; PEGylation; chitosan; nanoparticles; Thujone; brain targeting

ABSTRACT:

The goal of this study was to create biodegradable pegylated chitosan nanoparticles and assess how well they might target specific areas of the brain on a single platform. The PEGylated chitosan nanoconjugate was created and tested to transfer Thujone, a natural anti-Alzheimer constituent to the brain. Using the ionic gelation process, the nanoconjugate (TPNs) was created and assessed for a number of optical and in-vitro parameters. The Thujone loaded PEGylated nanosystem had IC₅₀ values of 0.42, 0.49, 0.67, and 0.75 μ M, according to the MTT experiment conducted on UCSD229i-SAD1-1 human astrocytoma cells. Enhanced uptake and biodistribution tests by confocal microscopy and apoptosis assay, which notably revealed increased accumulation of nanoconjugate in brain as compared to free Thujone solution, are authenticated by the in vitro cell lines evaluation. When compared to free Thujone solution, the targeting potential of TPNs was shown to be twice as significant. Conclusion: In order to improve the delivery of anti-Alzheimer medications to the brain for better treatment outcomes, bidoegradablePEGylated chitosan nanoconjugate may be employed as a possible nano-targeting to add PEGylated chitosan nanoparticles.

1. Introduction

One of the most complicated neurological conditions, Alzheimer's disease (AD) is a leading cause of severe dementia in the elderly. Decreased cognitive capacities resulting from cholinergic deficits are a hallmark of Alzheimer's disease (AD), a neurodegenerative disease that progresses over time [1]. Pathological markers such as neurofibrillary tangles, senile plaques, and neuronal and synaptic loss are used to further identify AD. Despite ongoing research, not all therapeutic targets or therapies have been found for AD; the disease's etiology remains unknown, and its medical demands remain

unfulfilled. The complexity of AD makes it challenging to create a viable treatment [2].

Unfortunately, a number of obstacles, including the blood-brain barrier (BBB), low bioavailability, or pharmacokinetic profile, prevented many therapeutically effective compounds for the treatment of AD from reaching the ideal pharmacological concentration. To address these issues, a number of alternative approaches have been proposed to transport drugs directly to the brain, including high dose therapy and the creation of drug carrier systems such liposomes, nanoparticles (NPs), or chemical delivery systems [3–4].



Biodegradable polymeric nanoparticles (NPs) are one of the innovative drug release strategies that have drawn attention as a promising drug delivery system (DDS) for neurological diseases because of their ability to both deliver a variety of therapeutic molecules to the targeted region for sustained, controlled, and/or site-specific release, as well as to protect the drug while transporting it to the damaged brain area. Polymeric nanoparticles have received a lot of attention lately as a potential medication delivery vehicle [5]. One definition of a nanoparticle is a submicron drug-carrier system, usually made of polymers. The medications or other molecules can be connected, entrapped, encapsulated, adsorbed, or dissolve into the nanoparticles.

These systems are appealing since the preparation techniques are typically straightforward and scalable. Numerous substances, including polysaccharides, copolymers, gelatin, albumin, and PEG (polyethylene glycols), can be used to create nanoparticles. Additionally, nanoparticles are essential for therapeutic targeting [6-7]. It is evident that a multitude of medication delivery methods can be employed to distribute nanoparticulate carriers. Drugs that are hydrophilic or hydrophobic, proteins, vaccinations, and biological macromolecules can all be delivered using nanoparticles. N-acetylglucosamine and glucosamine copolymers make up chitosan. Due to its weak base nature, chitosan is soluble in diluted aqueous acidic solution (pH less than 6.5) but insoluble in water and organic solvents [8].

In alkaline solutions, it precipitates and gels at lower pH levels. Chitosan is mucoadhesive and has a positive charge in contrast to many other polymers. Moreover, it has antimicrobial, biodegradable, and biocompatible properties [9]. In accordance with the historical roots of pharmaceutical research, plants possessing active ingredients are emerging as novel potential treatments for Alzheimer's disease. Plant active secondary metabolites work in concert with other components from the same plant to counteract the harmful effects of AChE and BChE, in addition to neutralizing the poisonous effect of chemicals. Many plants have been utilized to treat various neurological conditions, such as neurodegenerative disorders and neuropharmacological disorders, according to the history of drug development [10-11].

The herb *Salvia officinalis* is isolated Thujone is frequently used in traditional medicine to treat neuropathy, lung and urine infections, cancer, blood pressure reduction, improved digestion, and premature ejaculation. It is also used as a disinfectant. Colloidal carriers, particularly those composed of mucoadhesive polymers, are of particular interest among the various strategies investigated thus far since they guarantee drug time retention at the absorption site [12-13]. In this work, a natural *Salvia officinalis* derived Thujone was included using glucosamine-anchored PEGylated Chitosan nanoparticles as a stable and safe vehicle for brain targeting against Alzheimer disease.

Few reports have been made about the use of chitosan combined with the isolated Thujone from *Salvia officinalis* as a nanotherapy technique to treat Alzheimer's disease. Through ligand-oriented brain targeting that may have synergistic effects, we have shown in this study the increased targeted efficiency of PEGylated nanoparticles to include these extracts and bring about significant benefits against Alzheimer's disease [14-15].

2. MATERIALS AND METHODS

2.1 Collection and Authentication of Plant Material

The isolated pure Thujone continent was purchased from The Ayurveda medicologycenter, Bengaluru, Karnataka, India. Additionally, we bought sodium tripolyphosphate (TPP) and low molecular weight chitosan from Sigma Aldrich (Lisbon, Portugal). For the low molecular weight (LMW) CS, the degree of deacetylation was 85%, and the purity grade was 85%. We bought pure acetic acid from Ponalab in Lisbon, Portugal. Merck supplied the hydrochloric acid (HCl) and sodium hydroxide (NaOH) (Darmstadt, Germany). Using Millipore water purification technology (Millipore, Billerica, MA), ultra-pure water was produced in the lab.

2.2 Preparation of Nanoparticles and PEGylated process

The isolated Thujone was meticulously encapsulated during the production of chitosan using the ionotropic gelation process. Glacial acetic acid (GAA) solution containing 1% v/v and 100 mg of accurately weighed Thujone and 0.4% w/v chitosan were dissolved in it. At



a rate of 2 milliliters per minute (12 milliliters of TPP in 20 milliliters of drug polymer solution), 0.4% sodium tripolyphosphate solution (TPP) was added drop wise to the drug polymer solution [16]. To obtain nano-sized particles, the resultant particle dispersion was subjected to sonication using a probe sonicator (S-4000; Misonix, Farmingdale, NY) at medium amplitude (50%) for five minutes. In order to ensure maximum transportation at the intended site, the dispersion was next filtered using a 0.2 μm hydrophilic filter (Minsart, Sartorius) to isolate smaller nano size particles [17].

The resulting nanoparticles were then meticulously refined using ultrafiltration (Amicon 8200 against double-distilled water at the ideal temperature, using a millipore PBMK membrane, MWCO 300000). Ultrafiltration makes it easier to get rid of leftover unreacted solvent and unbound medication. In order to perform the PEGylation process, precisely 50 mL of 0.3% chitosan nanoparticles were added in a 3:1 ratio to a polyethylene glycol (PEG) solution, and the mixture was agitated for one hour at 500 rpm. To create homogenous PEG-Chitosan nanoparticles, the mixture was further treated to dispersion for 60 seconds [18].

3. Characterization

3.1 Particle size, Zeta potential, pH and Morphology

The Malvern Zetasizer 3000 particle size and zeta potential analyzer (Malvern Instruments, Bedfordshire, UK) was used to measure the developed TPNs, particle size, and surface charge. By smearing the electrophoretic mobility of particles in an applied electrical field, the Zeta potential of TPNs was investigated [19]. For prospective evaluation, the concentration of TPNs nanoformulation was adjusted to 0.01% w/v using pure water or in a 0.01 M sodium chloride solution. A digital pH meter (HI-TECH WATER TECH, New Delhi, India) was used to calculate the pH. After the pH meter was first calibrated using a buffer tablet, it was post-calibrated by dipping it in a beaker containing TPNs nanoformulation [20]. The measurement was done three times, the nanoformulation was evaluated in triplicate, and an average value with standard deviation was given.

3.2 Dynamic Light Scattering (DLS)

The Brook-heaven BI 9000 AT instrument (Brookhaven Instrument Corporation, USA) was utilized to investigate mean diameter and PDI of the TPNs nanoformulation by Dynamic Light Scattering (DLS). The more accurate and meaningful assessment of TPNs nanoformulation was determined using the DLS examination. For TPNs and nanoformulation, the DLS evaluation was carried out at wavelength 417 at a temperature of 25°C [21].

3.3 Transmission Electron Microscopy (TEM)

To measure the TEM of the TPNs nanoformulation, a Hitachi H-7500 TEM analyzer was used. To visualize the form and structure of the nanoformulation, TEM metaphors were created. After being put in a copper disc grid, the TPNs nanoformulation was coated with 2.5% w/v of phosphor-tungstic acid (PTA) solution [22]. After that, the grid was dried out using a 60-watt LED lamp (Philips, India Ltd.), put into the disc holder, and scanned for TEM analysis.

3.4 Scanning Electron Microscopy (SEM)

Using a German SEM, the Nova Nano SEM 450, the morphology and structure of the prepared TPNs nanoformulation were examined. The formulations were lyophilized using a freeze-dry lyophilizer (REMI, New Delhi, India) prior to the SEM examination. Then, using dual adhesive tape at 50mA for 5–10 minutes via sputter (KYKY SBC-12, Beijing, China), the dried formulations were mounted on a SEM stub [23]. The produced TPNs nanoformulation was digitally imaged using a SEM assisted by a secondary electron detector.

3.5 Entrapment Efficiency (EE):

In order to provide the desired therapeutic benefit, EE is crucial in delivering the bioactive to the intended location at the precise therapeutic dose. The pellets from the nanoformulation were obtained by centrifuging it for five minutes at 10,000 rpm in order to quantify the EE. The drug content was measured spectrophotometrically using a UV spectrophotometer (Schimadzu, Japan) set to 317 nm for TPNs nanoformulation in comparison to a blank solvent after the collected supernatant had been thoroughly diluted with PBS of pH 7 [24]. The following formula can be used to calculate the EE:



$$EE = \frac{\text{weight of drug in nanoformulation}}{\text{weight of drug taken}} \times 100$$

3.6 In vitro Drug Release studies

To forecast the diffusion and kinetic behavior of the nanosystem for the intended therapeutic efficiency, the release from the TPNs nanoformulation was monitored. The TPNs that were left over after centrifugation were suspended in 10 milliliters of a pH 7.4 phosphate buffered saline (PBS) solution for release tests [25]. After being transferred to a clean Eppendorf tube, the nanoparticle suspension was stirred and kept in a water bath at 37 °C. Samples were taken out of the bath after 0.5, 1, 2, 4, 6, and 24 hours, and they were centrifuged for five minutes at 14,000 rpm (BOECO, Hamburg, Germany). The amount of medication released from the nanoparticles over the allotted time was determined by UV spectroscopic analysis of the supernatants [26]. Every time, samples were examined in triplicate.

3.7 Cell Line studies

3.7.1 Cell Culture and Harvesting

The NCCs in Pune provided the Human UCSD229i-SAD1-1 human astrocytoma cell line, which was preserved in Dulbecco's modified Eagles Medium. Next, 10% fetal bovine serum (FBS), 100 U/mL penicillin, and 100 µg/mL streptomycin (PAA Laboratories GmbH, Austria) antibiotic solution were added to the cell line. The UCSD229i-SAD1-1 cell line was grown in 75 cm² tissue culture flasks and kept at 37°C in an environment with 5% CO₂. The cells were trypsinized using 0.25% trypsin EDTA solution (Sigma, USA) once they reached 90% confluency. The UCSD229i-SAD1-1 cells were seeded at a density of 50,000 cells per well in a 6-well plate (Costars, Corning Inc., NY, USA) for additional statistically qualitative analysis of cell uptake and apoptosis [27].

3.7.2 Cell uptake Assay by CLSM

UCSD229i-SAD1-1 cell lines were used in the qualitative cell uptake assay to test the nanoformulation's dispersal capabilities using confocal laser microscopy (CLSM). For three hours, the cells were grown using TPNs formulation and free Thujone solution, which is equivalent to one microgram per milliliter. Following the gestation period, the formulation-containing media were detected using an

Olympus FV1000 CLSM after three rounds of washing with Hanks buffered salt solution (PAA Laboratories GmbH, Austria) [28].

3.7.3 MTT Assay

In order to perform the MTT assay, the UCSD229i-SAD1-1 cell line was seeded in 96-well plates and cultured in media containing TPNs, free Thujone solution (equivalent concentrations of 0.1, 1, 10, and 20 µg/mL), normal saline solution-treated cells as the negative control, and Triton X-100 as the positive control [29]. Following a 24-hour gestation period, the medium containing the samples were dissected, and the cells underwent three rounds of HBSS washing. Then, each well received 150 µL of the MTT solution (500 µg/mL in PBS), which was added and incubated for an additional four hours. Following four hours, the formazan crystals were dissolved in 200 microliters of DMSO after the MTT solution had been articulated. After that, an ELISA plate reader (Bio Tek, USA) was used to screen the resulting solution's optical density (OD) at 570 nm [30].

3.7.4 Apoptosis Analysis

The ability of the TPNs formulation and free Thujone solution to cause apoptosis in UCSD229i-SAD1-1 cell lines was used to measure their cell cytotoxicity. The phosphatidyl serine discovery of the plasma membrane's outer layer and its interaction with Annexin V is the basis for the Annexin V apoptosis assay [31]. In a nutshell, UCSD229i-SAD1-1 cell lines were sown in a 6-well cell culture plate and stored at 37°C and 5% CO₂ for the entire night. After that, the media was clarified and replaced with one that included the TPNs formulation together with free Thujone solution (10 µg/mL), and it was allowed to gestate for six hours.

Following incubation, the media was enunciated, the cells were treated with 6-carboxyfluorescein di-acetate (6-CFDA) Annexin V Cy3™ Apoptosis Detection kit, Sigma, USA, and Annexin V Cy3.18 (AnnCy3). The cells were also washed three times with HBSS. Afterwards, using CLSM, the UCSD229i-SAD1-1 cell was seen in the green and red channels for 6-CFDA and AnnCy3, respectively [32]. Additionally, the fluorescence strength ratio of the green channel, which indicates vitality, to the red channel, which indicates



apoptosis, was analyzed to determine the Apoptosis index. The U.S. National Institutes of Health, Bethesda, Maryland, USA, Image j program was used to estimate the fluorescence signals in the photographs.

By dividing the percentage of apoptotic cells (annexin+) by the total percentage of cells in the sample (apoptotic [annexin+] plus no apoptotic cells [annexin-]), one can compute the apoptotic Index (AI). The apoptotic index was computed using the following formula:

$$AI = \frac{\%AV+C}{(\%AV+C + \%AV-C)}$$

Where %AV+C represent the percentage of annexin V positive cell and %AV-C represent the percentage of annexin V negative cells [33].

3.8 Statistical analyses

The mean \pm SD was used to express the values. Data. One-way analysis of variance (ANOVA) was used to statistically analyze the data using origin software; a value of $p < 0.01$ was deemed significant for $n = 3$ [34].

4 Results & Discussion

As soon as the pawn anion TPP was combined with the consistent chitosan polymer solutions, the natural Thujone obtained from *Salvia officinalis* was ensnared by PEGylated chitosan nanoparticles. Ionic interactions between the positively charged amino groups of chitosan and the negatively charged ion TPP led to the production of nanoparticles. In order to achieve stable dispersion and the production of nanoscale particles, the CS/TPP ratio was tuned. Initial tests were conducted to determine the ideal CS and TPP concentrations for NP production. To produce physiochemically and thermally stable nanoparticles, the formulation and process parameters were carefully tuned. The resulting nanoparticles were classified as an aggregate, an opalescent suspension showing a Tyndall effect (TNPs), or a transparent solution.

4.1 Particle size, Zeta Potential and Morphology

The generated TPNs formulations with sizes ranging from 150 to 200 nm were clearly distinguished by the

zeta sizer measurement results (Figure 1-a). Because of the formulation and process optimization, the TPNs formulations' nano size showed respectable bio constituent encapsulation in the polymer matrix. The synthesized nanoformulation TPNs was discovered to have a negative charge, as evidenced by its surface charge of -12.22 mV (Figure 1-c). Better stability and optimal candidacy for improved brain targeting were demonstrated by the formulation's negative charge. The pH of the TPNs nanoformulation was found to be 6.4 ± 0.12 , which is important for delivering the drug to almost neutral microenvironments for effective brain targeting. The primary component of the onsite breakdown of the polymer matrix is the pH assisted targeting mechanism. The intended therapeutic potential was achieved by enhancing drug release at a controlled rate through the activation mechanism of polymeric breakdown.

4.2 DLS Analysis

The prepared TPNs nanoformulation's nanosize range dispersion is again determined using the DLS. The ideal nanosize range of 160–240 nm for improved BBB crossing is represented by a nearly similar size distribution pattern in the produced nanoformulation. The produced nanoformulation's ideal nanosize range showed improved brain delivery and onsite targeting that effectively complies with the size of cells and their microenvironment. Diverse size distributions and dispersion patterns were revealed by the DLS research. The PDI that TPNs displayed was determined to be 0.243 ± 0.13 . The produced nanoparticles between 100 and 500 nm had an equal size distribution pattern and improved stability, according to the DLS data (Figure 1-b). When brain targeting, this constant pattern of nanosize makes it easier for prepared nanoparticles to diffuse across blood-brain barriers and reach their maximum pharmacological potential. It is so unequivocal to say that the created nanoformulation shown ideal and consistent nano dispersion characteristics for the operational brain targeting against Alzheimer treatment in a clinical platform.

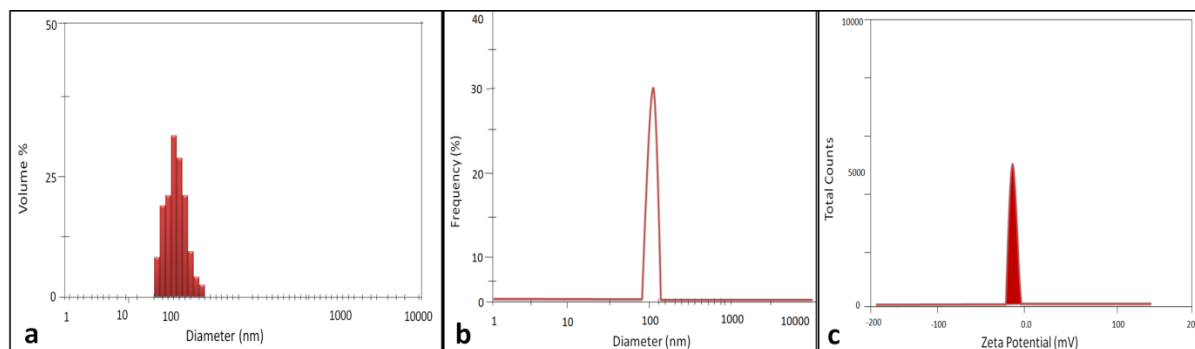


Figure 1: Image (a) showing zeta sizer evaluated particle size and distribution pattern of developed TPNs nanoformulation, whereas images (b) displaying dynamic light scattering diameter of TPNs nanoformulation. Image c showing zeta potential of developed TPNs formulation, (mean \pm SD, n=3).

4.3 Transmission Electron Microscopy (TEM)

The produced nanoformulation TPNs oval-shaped nanoparticles were revealed by the TEM investigation to be extremely discrete in size. The TEM examination for TPNs revealed a size range of 100-200 nm, which is consistent with the DLS measurement zeta sizer analysis (Figure 2-a). The entrapment of natural isolated constituent resulted in nanoparticle production that demonstrated improved crosslinking between the polymer and cross linker, preventing undesired leakage. Additionally, it was discovered that there was very little nanoparticle agglomeration, indicating improved chitosan boundary PEGylation. The transencephalogram (TEM) results indicated that the two nanoformulations had a respectable appearance of BBB infiltration and a viable nano carrier system for efficient brain delivery.

4.4 Scanning Electron Microscopy (SEM)

The results of the TEM assay and zeta sizer, which demonstrate the generation of tiny particles with smooth morphology and spherical shape, were greatly improved by the SEM examination. The SEM pictures clearly show that the developed nanoformulation with improved PEGylation technique has strong oval borders. The SEM pictures also make clear that there is no evidence of cluster formation or particle aggregation with a noticeable PEG outer layer. The generated TPNs optimal brain targeted delivery features were further confirmed by the zeta-sizer analysis, and the SEM analysis results showed a size range of 120-200 nm, qualitatively verifying the TEM (Figure 2, b).

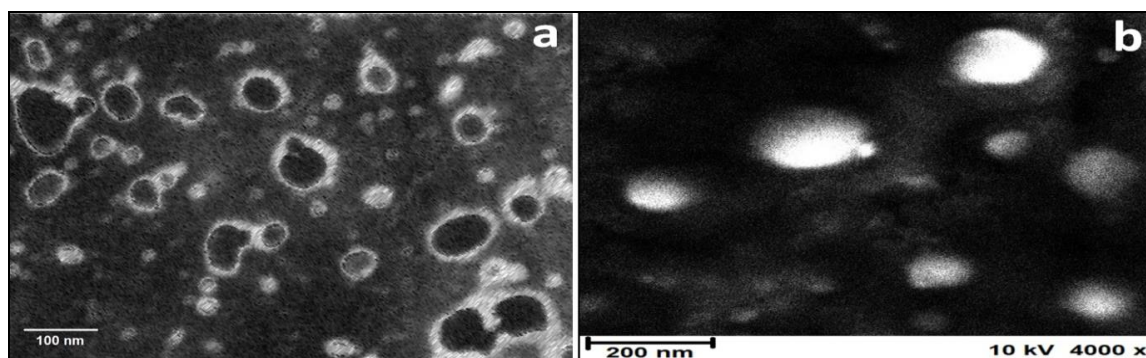


Figure 2: Image a & b showing Transmission electron microscopy (TEM) and Scanning electron microscopy (SEM) of developed TPNs nanoformulation at 100 and 200 nano scale resolution respectively, (mean \pm SD, n=3).



4.5 In-vitro drug release studies

Figure 3(a) showing in vitro drug release data of Thujoneloaded with PEGylated nanoformulation. A non-linear release profile, marked by a considerably rapid initial drug release over the first 3–4 hours, followed by a slower release in the latter period, was seen in the drug release pattern from the produced nanoformulation TPNs at different pH values (4.0 & 7.4). In order to thoroughly assess the impact of nanoformulation for improved brain targeting and onsite delivery, two pH ranges were supplied. By using nanoformulation, the biphasic drug release pattern was observed, with the first 8 hours of the release being a gradual release followed by the first 8 hours of nanoparticle bursting. According to in-vitro drug release tests, TPNs first allowed for burst release of the drug constituent at a pH of 4.0. It was discovered that the drug release for TPNs was $87.22 \pm 1.67\%$ at 6 hours, 89.54 ± 3.07 at 8 hours, 90.11 ± 2.29 percent at 6 hours, and $93.65 \pm 3.56\%$ at 8 hours. Conversely, at pH 7, the drug release from TPNs was considerably ($P < 0.05$) delayed after 24 hours. Therefore, at 24 hours into the experimental drug release phenomena, the release rate of bio constituent for TPNs was shown to be considerable.

4.6 In vitro cellular uptake

UCSD229i-SAD1-1 human astrocytoma cell line was used to assess and quantify the produced nanoformulation TPNs ability to target cells and transport intracellularly. The human astrocytoma cell line is a crucial component of the blood-brain barrier and is often used to study brain delivery. When assessed by CLSM analysis, the created TPNs demonstrated notable cellular uptake and circulation in comparison to

the free drug Thujone solution. When treated with Rhodamine B isothiocyanate (RITC), the generated TPNs CLSM signals were more robust and crisp, exhibiting enhanced absorbance when compared to the free drug Thujone solutionsolution after 12 hours of incubation (Figure 4).

Furthermore, the nanoformulation's bright fluorescent signals revealed by confocal laser scanning microscopy clearly indicated the vesicular localization of the nanoparticles, indicating enhanced advancement of the endocytic pathway. In vitro cellular uptake and resilience were shown to be twice as high with TPNs in comparison to freeThujone solution on brain cell membranes, according to the results of the CLSM intensity examination. Following a 12-hour incubation period, the Thujone solutiontreated cells were also quantitatively observed using inductively attached plasma optical emission (ICP-OE) spectrometry.

The transwell assay at the basolateral side validates the results, which effectively indicate that around ~45% of TPNs and ~13% of the free Thujone solutionnanofomulation have sharply penetrated into the BBB layer. Due to early adsorption at the cell membrane that limits direct diffusion to the cells, the free Thujone solutiondemonstrated scarce diffusion across the BBB via UCSD229i-SAD1-1 human astrocytoma cells of around 13%, indicating non-significant intracellular transport and penetrating efficiency. Overall, at various incubation times, TPNs cell uptake and transportation capacity outperformed free drug Thujone solutionwith bright fluorescent advertisements, regardless of any morphological variations in cell lines, leading to improved brain targeting efficacy.

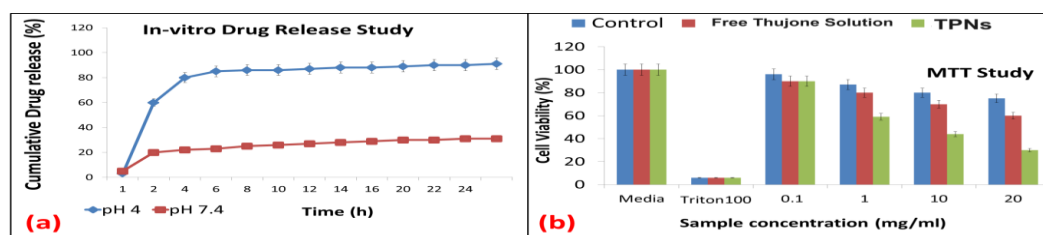


Figure 3: Image a showing drug release kinetics of developed TPNs at pH 4 and 7 using dialysis bag membrane, whereas image b elaborating MTT cell cytotoxicity assay of developed TPNs nanoformulation at different concentration, (mean \pm SD, n=3).

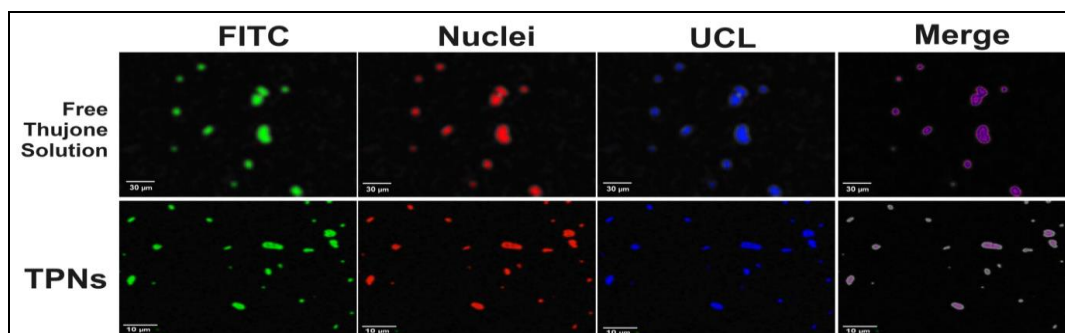


Figure 4: Elaboration of in-vitro cellular uptake and CLSM localization analysis on UCSD229i-SAD1-1 human astrocytoma cells line by developed TPNs and comparing with free Thujone solution at 30µm scale bar after 12 h incubation respectively, * $p < 0.05$ and * $p < 0.01$ compared to the untreated cell, (mean + SD, n=3),

4.7 In vitro cytotoxicity assay

The generated TPNs nanoformulation was investigated in relation to UCSD229i-SAD1-1 human astrocytoma cells using the MTT assay. After a 24-hour incubation period, the MTT assay qualitatively demonstrated the nanoformulation's strong anti-proliferation potential. The studies demonstrated that the normal control group (saline solution) had 100% cell viability, while the negative control group (Triton X 100 surfactant solution) had 10% cell viability. After 24 hours of incubation, the produced TPNs demonstrated noteworthy cell viability of 94%, 87%, 72%, and 66% at varied concentrations (0.1, 1, 10, and 20 µg/mL of individual concentration) (Figure b). In contrast, after 24 hours of incubation, the free Thujone solution demonstrated cell viability of 97%, 80%, 59%, and 38%.

The MTT study demonstrated a nonlinear relationship between incubation time and anti-proliferation efficiency by demonstrating non-significant cell cytotoxicity by various substances after 24 hours of incubation. The MTT results unmistakably showed that, after 24 hours of incubation, the nanoformulation significantly increased cell viability over Thujone solution, indicating biologically safe brain targeting efficiency with little toxicity on human astrocytoma cells. Better physicochemical compatibility between the nanocomposite, which leads to effective cellular transport and brain administration, is the cause of the increased cell viability demonstrated by the developed TPNs. When comparing the nanoformulation with free drug Thujone solution, TPNs has a higher cell survival

and less cell cytotoxicity at higher concentrations than the free drug Thujone solution. Better endocytosis and robustness of TPNs were demonstrated by the intercomparison results, which were determined to be statistically significant when examined using the student's T test. Overall, the results of the cell toxicity tests make it abundantly evident that the created nanocomposite may be utilized as a unique drug carrier that contains natural bio constituent and is intended to be used as a targeted delivery system for the treatment of brain disorders.

4.8 Apoptosis assay

The examination of apoptosis shown by free Thujone solution and the created TPNs confirmed apoptosis at all doses. When compared to the free drug Thujone solution, the produced TPNs displayed inherent apoptosis. It has been observed that both TPNs exhibited the phenomena of mitochondrial apoptosis or death activator through activation of cell surface receptor. The caspase cascade is activated by activating cell surface receptors, which sets optimal cell death and initiates the appropriate apoptotic process. The Thujone was shown to have an apoptosis index of 0.36 in free drug bio constituent, while the produced TPNs exhibited an apoptotic value of 0.69. When compared to ordinary free natural constituent, the nanoformulation demonstrated roughly two times greater apoptotic action, which was deemed to be significant (* $P < 0.01$) (Figure 5).

The main factor driving the nanosized particles' superior apoptosis over free drug constituent is their ability to facilitate faster onsite drug delivery, adequate



dispersion, and improved release. When the TPNs and free drug Thujone solution are compared, the student T test indicates that TPNs has a much higher apoptotic potential than the free drug solution. Overall, chitosan nanoparticles that have been pegylated have improved

circulation within the brain microenvironment, resulting in prolonged release and little drug toxicity, and improved brain targeting in the fight against Alzheimer's disease.

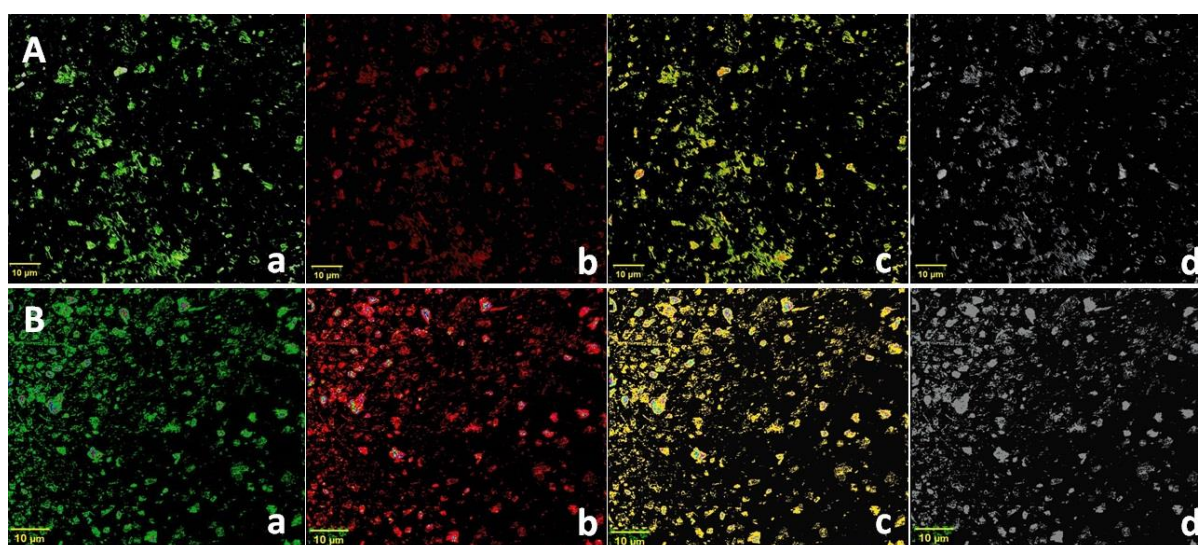


Figure 5: Images (A & B,) showing apoptosis assay of free Thujone solution and developed TPNs (10 µg/ml; 6h incubation) on UCSD229i-SAD1-1 human astrocytoma cells line; (a) Green channel depicts the fluorescence from carboxy fluorescein (cell viability marker dye); (b) Overlay image of figure (a) and figure (b); (c) Red channel depicts fluorescence from Annexin Cy3.18 conjugate (cell apoptosis marker dye); (d) depicted differential contrast image of representative cells. The apoptosis index measured as ratio fluorescence intensity from the red channel to that of green channel. The fluorescence intensities of the images were measured using Image J software, U. S. National Institutes of Health, Bethesda, Maryland, USA, <http://imagej.nih.gov/ij/>. (n=3, data expressed as average \pm SE, *denotes $p < 0.01$).

5 Summary and Conclusion

The Thujone constituent was effectively entrapped and studied in PEGylated chitosan-based nanoparticles in the current work using a modified ionic gelation technique to improve brain delivery. The first observation confirmed a stable optimization process that controlled the bio constituent release by altering the amount of medication and the polymer system's ideal size and percentage of encapsulated capacity. Several physiochemical techniques, including TEM and SEM, were used to precisely characterize the created nanoformulation system. Additionally, qualitative assessments were conducted to establish the creation of spherical shaped nanoparticles free from undesired

agglomeration. The in-vitro drug release mechanism demonstrated a prolonged release of drug from the nano vesicle for improved brain targeting, and the cytotoxicity assay demonstrated the nano formulation's remarkable cell survival at all concentrations. Through cell proliferation CLSM assessments, the in-vitro cyto-compatibility tests verify the enhanced absorption and dispersion of TPNs in the cell line with enhanced cell trans-cytosis signals. On the other hand, the novel brain targeting via natural bio constituent encapsulated biodegradable nano vesicle system, which offers advantages over conventional formulations such as low dose frequency, elevated bioavailability, and good patient compliance, is made possible by the recent developments in nanomedicine.



Acknowledgement

We are thankful to our Guide and all departmental participants for supporting me guiding me. We acknowledge Patel College of Pharmacy, Madhyanchal Professional University, Bhopal for kind support.

References

1. Villegas, C.; Perez, R.; Petiz, L.L.; Glaser, T.; Ulrich, H.; Paz, C. Ginkgolides and huperzine A for complementary treatment of Alzheimer's disease. *IUBMB Life* 2022, 74, 763–779.
2. Nirale, P.; Paul, A.; Yadav, K.S. Nanoemulsions for targeting the neurodegenerative diseases: Alzheimer's, Parkinson's and Prion's. *Life Sci.* 2020, 245, 117394.
3. Patil, R.P.; Pawara, D.D.; Gudewar, C.S.; Tekade, A.R. Nanostructured cubosomes in an in situ nasal gel system: An alternative approach for the controlled delivery of donepezil HCl to brain. *J. Liposome Res.* 2018, 29, 264–273.
4. Kell, D.B.; Heyden, E.L.; Pretorius, E. The Biology of Lactoferrin, an Iron-Binding Protein That Can Help Defend against Viruses and Bacteria. *Front. Immunol.* 2020, 11, 1221.
5. Länger, R.; Stöger, E.; Kubelka, W.; Helliwell, K. Quality standards for herbal drugs and herbal drug preparations—Appropriate or improvements necessary? *Planta Med.* 2018, 84, 350–360.
6. Li, Y.; Shen, Y.; Yao, C.L.; Guo, D.A. Quality assessment of herbal medicines based on chemical fingerprints combined with chemometrics approach: A review. *J. Pharm. Biomed. Anal.* 2020, 185, 113215.
7. Wightman, E.L.; Jackson, P.A.; Spittlehouse, B.; Heffernan, T.; Guillemet, D.; Kennedy, D.O. The acute and chronic cognitive effects of a sage extract: A randomized, placebo-controlled study in healthy humans. *Nutrients* 2021, 13, 218.
8. Newcombe, E.A.; Camats-Perna, J.; Silva, M.L.; Valmas, N.; Huat, T.J.; Medeiros, R. Inflammation: The link between comorbidities, genetics, and Alzheimer's disease. *J. Neuroinflammation* 2018, 15, 276.
9. Swerdlow, R.H. Mitochondria and mitochondrial cascades in Alzheimer's disease. *J. Alzheimer's Dis.* 2018, 62, 1403–1416.
10. Huat, T.J.; Camats-Perna, J.; Newcombe, E.A.; Valmas, N.; Kitazawa, M.; Medeiros, R. Metal toxicity links to Alzheimer's disease and neuroinflammation. *J. Mol. Biol.* 2019, 431, 1843–1868.
11. Chauhan, N.; Vasava, P.; Khan, S.L.; Siddiqui, F.A.; Islam, F.; Chopra, H.; Bin Emran, T. Ethosomes: A novel drug carrier. *Ann. Med. Surg.* 2022, 82, 104595.
12. Tenchov, R.; Bird, R.; Curtze, A.E.; Zhou, Q. Lipid Nanoparticles—From Liposomes to mRNA Vaccine Delivery, a Landscape of Research Diversity and Advancement. *ACS Nano* 2021, 15, 16982–17015.
13. Pashirova, T.N.; Zueva, I.V.; Petrov, K.A.; Lukashenko, S.S.; Nizameev, I.R.; Kulik, N.V.; Voloshina, A.D.; Almasy, L.; Kadirov, M.K.; Masson, P.; et al. Mixed cationic liposomes for brain delivery of drugs by the intranasal route: The acetylcholinesterase reactivator 2-PAM as encapsulated drug model. *Colloids Surf. B Biointerfaces* 2018, 171, 358–367.
14. Kaur, A.; Nigam, K.; Srivastava, S.; Tyagi, A.; Dang, S. Memantine nanoemulsion: A new approach to treat Alzheimer's disease. *J. Microencapsul.* 2020, 37, 355–365.
15. Kaur, A.; Nigam, K.; Bhatnagar, I.; Sukhpal, H.; Awasthy, S.; Shankar, S.; Tyagi, A.; Dang, S. Treatment of Alzheimer's diseases using donepezil nanoemulsion: An intranasal approach. *Drug Deliv. Transl. Res.* 2020, 10, 1862–1875.
16. Froelich, A.; Osmalek, T.; Jadach, B.; Puri, V.; Michniak-Kohn, B. Microemulsion-Based Media in Nose-to-Brain Drug Delivery. *Pharmaceutics* 2021, 13, 201.
17. Wen, M.M.; Ismail, N.I.K.; Nasra, M.M.A.; El-Kamel, A.H. Repurposing ibuprofen-loaded microemulsion for the management of Alzheimer's disease: Evidence of potential intranasal brain targeting. *Drug Deliv.* 2021, 28, 1188–1203.
18. Gartúa, D.E.; Martinez, C.S.; Alonso, S.D.V.; Prieto, M.J. Combined Therapy for Alzheimer's



- Disease: Tacrine and PAMAM Dendrimers Co-Administration Reduces the Side Effects of the Drug without Modifying its Activity. *AAPS PharmSciTech* 2020, 21, 110–114.
19. Ni, Y.-N.; Kong, L.; Li, X.-T.; Xiao, H.-H.; Wu, Y.-T.; Liang, X.-C.; Lin, Y.; Li, W.-Y.; Deng, Y.; Li, Y.; et al. Multifunctional osthole liposomes and brain targeting functionality with potential applications in a mouse model of Alzheimer's disease. *J. Liposome Res.* 2020, 31, 267–278.
20. Yusuf, M.; Khan, M.; Alrobaian, M.M.; Alghamdi, S.A.; Warsi, M.H.; Sultana, S.; Khan, R.A. Brain targeted Polysorbate-80 coated PLGA thymoquinone nanoparticles for the treatment of Alzheimer's disease, with biomechanistic insights. *J. Drug Deliv. Sci. Technol.* 2021, 61, 102214.
21. Zorkina, Y.; Abramova, O.; Ushakova, V.; Morozova, A.; Zubkov, E.; Valikhov, M.; Melnikov, P.; Majouga, A.; Chekhonin, V. Nano Carrier Drug Delivery Systems for the Treatment of Neuropsychiatric Disorders: Advantages and Limitations. *Molecules.* 2020, 25, 5294.
22. Haider, M.; Abdin, S.M.; Kamal, L.; Orive, G. Nanostructured Lipid Carriers for Delivery of Chemotherapeutics: A Review. *Pharmaceutics* 2020, 12, 288
23. Plaza-Oliver, M.; Santander-Ortega, M.J.; Lozano, M.V. Current approaches in lipid-based nanocarriers for oral drug delivery. *Drug Deliv. Transl. Res.* 2021, 11, 471–497.
24. Costa, C.P.; Moreira, J.N.; Lobo, J.M.S.; Silva, A.C. Intranasal delivery of nanostructured lipid carriers, solid lipid nanoparticles and nanoemulsions: A current overview of In Vivo studies. *Acta Pharm. Sin. B* 2021, 11, 925–940.
25. Tripathi, S.; Gupta, U.; Ujjwal, R.R.; Yadav, A.K. Nano-lipidic formulation and therapeutic strategies for Alzheimer's disease via intranasal route. *J. Microencapsul.* 2021, 38, 572–593.
26. Almuhayawi, M.S.; Ramadan, W.S.; Harakeh, S.; Al Jaouni, S.K.; Bharali, D.J.; Mousa, S.A.; Almuhayawi, S.M. The potential role of pomegranate and its nano-formulations on cerebral neurons in aluminum chloride induced Alzheimer rat model. *Saudi J. Biol. Sci.* 2020, 27, 1710–1716.
27. Topal, G.R.; Mészáros, M.; Porkoláb, G.; Szecskó, A.; Polgár, T.F.; Siklós, L.; Deli, M.A.; Veszélka, S.; Bozkir, A. ApoE-Targeting Increases the Transfer of Solid Lipid Nanoparticles with Donepezil Cargo across a Culture Model of the Blood–Brain Barrier. *Pharmaceutics* 2020, 13, 38
28. Liu, X.-G.; Zhang, L.; Lu, S.; Liu, D.-Q.; Huang, Y.-R.; Zhu, J.; Zhou, W.-W.; Yu, X.-L.; Liu, R.-T. Superparamagnetic iron oxide nanoparticles conjugated with A β oligomer-specific scFv antibody and class A scavenger receptor activator show therapeutic potentials for Alzheimer's Disease. *J. Nanobiotechnology* 2020, 18, 160.
29. Zhao, J.; Xu, N.; Yang, X.; Ling, G.; Zhang, P. The roles of gold nanoparticles in the detection of amyloid- β peptide for Alzheimer's disease. *Colloid Interface Sci. Commun.* 2022, 46, 100579.
30. Hou, K.; Zhao, J.; Wang, H.; Li, B.; Li, K.; Shi, X.; Wan, K.; Ai, J.; Lv, J.; Wang, D.; et al. Chiral gold nanoparticles enantioselectively rescue memory deficits in a mouse model of Alzheimer's disease. *Nat. Commun.* 2020, 11, 4790.
31. Ayaz, M.; Ovais, M.; Ahmad, I.; Sadiq, A.; Khalil, A.T.; Ullah, F. Biosynthesized metal nanoparticles as potential Alzheimer's disease therapeutics. In *Metal Nanoparticles for Drug Delivery and Diagnostic Applications*; Elsevier: Amsterdam, The Netherlands, 2020; pp. 31–42
32. Ling, T.S.; Chandrasegaran, S.; Xuan, L.Z.; Suan, T.L.; Elaine, E.; Nathan, D.V.; Chai, Y.H.; Gunasekaran, B.; Salvamani, S. The Potential Benefits of Nanotechnology in Treating Alzheimer's Disease. *BioMed Res. Int.* 2021, 2021, 5550938
33. Revi, M. Alzheimer's Disease Therapeutic Approaches. In *GeNeDis 2018: Genetics and Neurodegeneration; Advances in Experimental Medicine and Biology*; Springer: Berlin/Heidelberg, Germany, 2020; pp. 105–11
34. Passeri, E.; Elkhoury, K.; Morsink, M.; Broersen, K.; Linder, M.; Tamayol, A.; Malaplate, C.; Yen, F.T.; Arab-Tehrany, E. Alzheimer's Disease: Treatment Strategies and Their Limitations. *Int. J. Mol. Sci.* 2022, 23, 13954